AIMS Materials Science, 13(1): 168–186.
DOI: 10.3934/matersci.2026010
Received: 26 November 2025
Revised: 28 January 2026
Accepted: 03 February 2026
Published: 27 February 2026

https://www.aimspress.com/journal/Materials

Research article

Microwave deicing efficiency and microwave loss characteristics of carbon nanofibers reinforced concrete

Zhihang Wang[1,*], Binghong Li[1], Chao Zhang[1], Yue Zhang[1], Chao Wang[1] and Erlei Bai[2]

[1] Air Force Logistics Academy, Jiangsu 221000, China
[2] Aviation Engineering School, Air Force Engineering University, Xi'an 710038, China

* **Correspondence:** Email: songchenwzh@163.com.

Abstract: In this work, the ice-free heating test and microwave deicing test of carbon nanofiber (CNFs)-reinforced concrete (CNFsRC) were carried out, and the effect of CNFs on the temperature rise rate, temperature distribution, and microwave deicing efficiency of concrete was studied. Also, the resistance loss and dielectric loss characteristics of CNFsRC were studied by measuring the resistivity and electromagnetic parameters of concrete. In addition, the microwave deicing efficiency and loss characteristics of CNFsRC and carbon fiber (CFs)-reinforced concrete (CFsRC) were compared. The results show that CNFs can improve the resistance loss and dielectric loss characteristics of concrete, so that the microwave deicing efficiency of CNFsRC is improved. As the CNFs content increases, the surface temperature, temperature rise rate, area of microwave heating region, and area of ice-breaking region of CNFsRC increase. CNFs can reduce the resistivity of concrete and increase the complex permittivity real part, imaginary part, and dielectric loss angle tangent. As the CNFs content increases, the microwave loss characteristics of CNFsRC increase. Compared with CFs, CNFs have better improvement in the microwave deicing efficiency of concrete. The resistance loss characteristics of CFsRC are better than those of CNFsRC, but the microwave absorption efficiency of CFsRC is poor, and the dielectric loss characteristics of CNFsRC are better than those of CFsRC.

Keywords: concrete; carbon nanofibers; carbon fibers; microwave deicing; microwave loss characteristics

1. Introduction

Highway pavement and airport pavement in cold regions are often affected by ice and snow. Ice and snow cover affect the friction coefficient and roughness of the pavement surface, thus reducing skid resistance and increasing traffic accidents [1,2]. Research has shown that traffic accidents caused by ice freezing on pavement account for more than 35% of the total traffic accidents in winter [3,4]. Therefore, removing ice and snow efficiently and quickly to ensure clear traffic is of great significance. Currently, snow removal technology on pavement surfaces is well-developed, but ice removal from pavement surfaces remains relatively difficult. Existing deicing methods include manual methods, mechanical methods, snow melting agents, and thermal melting methods [5]. Among those, manual methods, mechanical methods, and snow melting agents present some disadvantages, such as low ice removal rate, low operating efficiency, and serious damage to pavement structure [6,7]. Thermal melting methods have the advantages of environmental protection, high efficiency, and thorough deicing [8,9]. Therefore, the thermal melting method has become the research focus.

Among thermal melting methods, microwave deicing technology can significantly improve the ice removal rate, without resulting in environmental pollution or structural damage, with broad development prospects and promotion value [10,11]. However, microwave heating efficiency has become a key limitation on the application of this technology. The traditional pavement concrete has low microwave absorption efficiency and slow deicing speed [12,13]. Therefore, researchers have conducted several studies to improve the microwave absorption efficiency of plain concrete (PC) by wave-absorbing admixtures [14,15]. Zhang et al. found that rubber powder could improve the dielectric properties, and rubber powder–modified concrete showed better microwave heating rate [16]. Liu et al. studied the microwave deicing efficiency of iron black–modified concrete and found that when the iron black content was 15%, the wave absorption effect of concrete nearly doubled [17]. Chen et al. found that silicon carbide, Fe_4O_3 and graphite can improve the wave absorption effect of concrete, and Fe_4O_3 had the best improvement effect [18]. Liu et al. found that graphite could improve the microwave loss characteristics and deicing efficiency of concrete [19]. The above studies mainly focus on powder wave–absorbing admixtures, while there are relatively few studies on microwave heating efficiency of concrete modified by fiber wave–absorbing admixtures [20,21]. In addition, powder wave–absorbing admixtures easily deteriorate the mechanical properties of concrete because they do not participate in cement hydration [22,23], while fibers are often used to improve its mechanical properties [24]. Therefore, it is necessary to explore the effect of fiber wave–absorbing admixtures on the microwave heating rate of concrete.

Carbon-based fibers have excellent electromagnetic properties and are suitable for use in fiber wave–absorbing admixtures. Ren et al. and Meng et al. carried out some useful explorations on the microwave dicing efficiency of carbon fiber (CFs)-reinforced concrete (CFsRC) [25,26]. The former mainly focused on the coupling effect of the length and content of CFs on the ice-free heating efficiency of CFsRC, while the latter studied the temperature change of CFsRC during ice-free heating. Neither work involved the actual deicing effect and microwave loss characteristics of CFsRC. Improvements in microwave heating rate are essentially caused by the change in the microwave loss characteristics of concrete [27]. Therefore, it is necessary to explore the microwave heating rate and loss characteristics of concrete together. In addition, carbon nanofiber (CNFs) is a fibrous nanomaterial that can improve both mechanical properties and durability, such as

impermeability and frost resistance, of concrete [28,29]. The use of microwave deicing technology will improve the frequency of concrete freeze-thaw, which will impose higher requirements on the durability of concrete [30]. CNFs are also often used as resistance loss and dielectric loss materials to improve the wave-absorbing properties and electromagnetic shielding properties of composites [31,32]. Therefore, CNFs show great potential in improving the microwave heating rate of concrete.

In view of this, this study takes carbon nanofiber-reinforced concrete (CNFsRC) as the research object and carries out an ice-free heating test, microwave deicing test, resistivity test, and electromagnetic parameter test. Additionally, the temperature rise rate, temperature distribution, microwave deicing efficiency, resistance loss characteristics, and dielectric loss characteristics of CNFsRC are studied. In addition, the microwave deicing efficiency and loss characteristics of CNFsRC and CFsRC are compared.

2. Materials and methods

2.1. Preparation of the specimen

Materials include P·O 42.5 cement, limestone gravel (5–20 mm), natural river sand, water, polycarboxylate water reducer, and carbon-based fibers. Carbon-based fibers include CNFs and CFs, as shown in Figure 1; the main parameter indicators of CNFs and CFs are shown in Table 1. Three different sizes of concrete specimens are prepared, and the specimen working conditions are shown in Table 2.

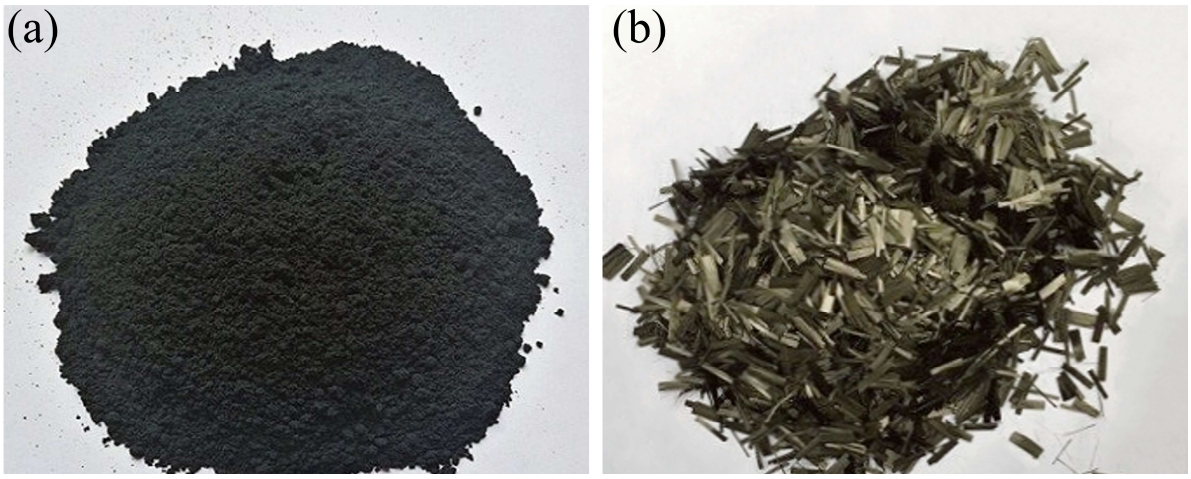

Figure 1. (a) CNFs and (b) CFs.

Table 1. Main parameter indicators of CNFs and CFs.

Carbon-based fibers	Diameter (μm)	Density (kg·m^{-3})	Resistivity (Ω·cm)	Length (μm)
CNFs	150–200 × 10^{-3}	180	0.01	10–20
CFs	7	1760	1.6 × 10^{-3}	9 × 10^{3}

Table 2. Specimen working conditions.

Test type	Specimen size	Age
Ice-free heating test	500 × 500 × 50 mm^3	28 d
Microwave deicing test	500 × 500 × 50 mm^3	
Resistivity test	100 × 100 × 400 mm^3	
Electromagnetic parameter test	108.2 × 53.6 × 40.0 mm^3	

The mix ratio of CNFsRC and CFsRC is shown in Table 3, where PC represents plain concrete, CNFsRC1–CNFsRC4 represent CNFsRC with CNF contents of 0.1%–0.4%, and CFsRC1–CFsRC4 represent CFsRC with CFs contents of 0.1%–0.4%. Before the preparation of concrete specimens, the uniformly dispersed fiber suspension is prepared using an ultrasonic instrument, and the preparation of CNF and CF suspensions and CNFsRC and CFsRC specimens is shown in Figure 2.

The specimen used for the microwave deicing test is required to freeze the ice on the concrete surface, as shown in Figure 3, as follows: (1) use an expandable polyethylene foam board as the ice-making mold and cut a section of 50 × 50 × 6 cm in the middle of the foam board; (2) put the concrete specimen in the mold, and install the temperature sensor; (3) put the mold into the refrigeration cabinet at −15 °C, inject water with a layer of 10 mm, and freeze for 8 h.

Table 3. Mix ratio of CNFsRC and CFsRC (kg/m^3).

Specimen No.	CNFs	CFs	Cement	Sand	Water	Gravel	Water reducer
PC	-	-	320	626	96	1456	3.52
CNFsRC1	0.18	-	320	626	96	1456	3.52
CNFsRC2	0.36	-	320	626	96	1456	3.52
CNFsRC3	0.54	-	320	626	96	1456	3.52
CNFsRC4	0.72		320	626	96	1456	3.52
CFsRC1	-	1.76	320	626	96	1456	3.52
CFsRC2	-	3.52	320	626	96	1456	3.52
CFsRC3	-	5.28	320	626	96	1456	3.52
CFsRC4		7.04	320	626	96	1456	3.52

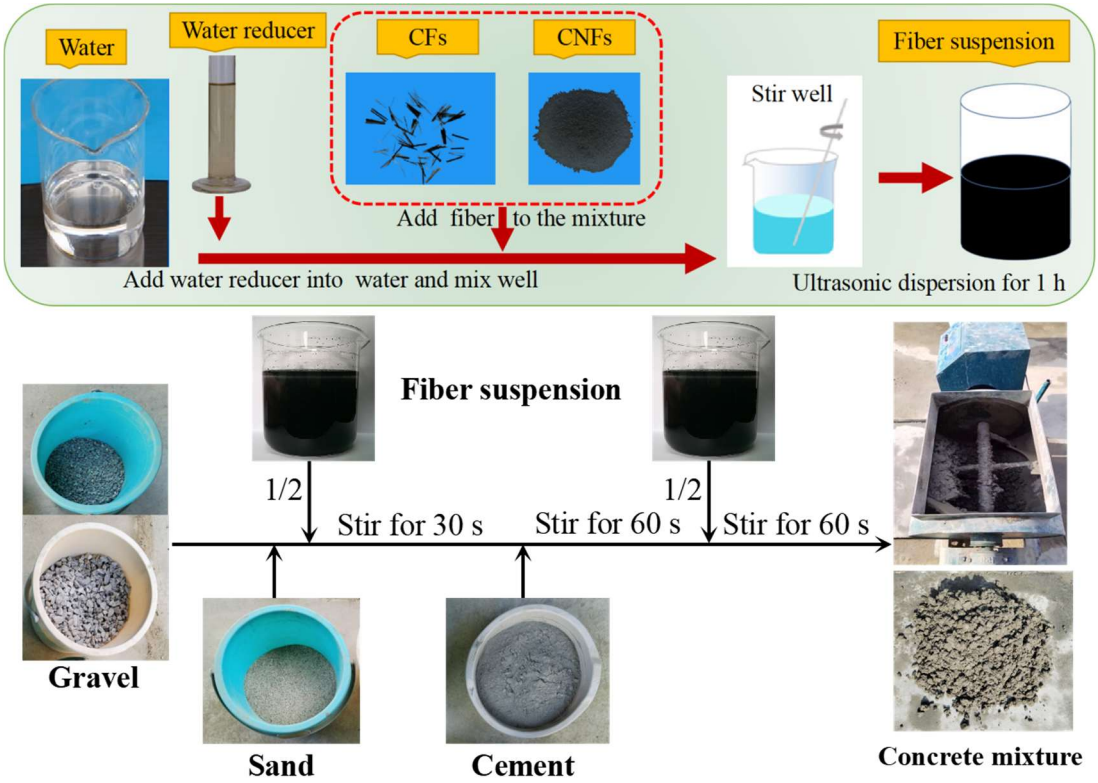

Figure 2. Preparation of CNF suspension, CF suspension, CNFsRC specimen, and CFsRC specimen.

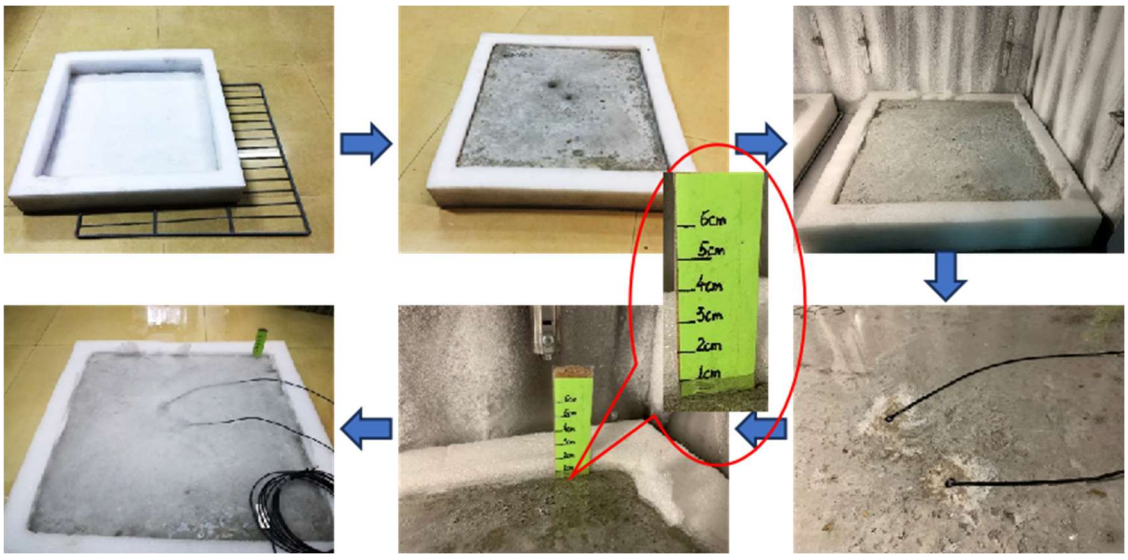

Figure 3. Preparation of the ice layer.

2.2. Test equipment

2.2.1. Open microwave deicing system

The open microwave deicing system is comprised of the energy device, microwave radiation device, control device, and temperature measurement device [33], as shown in Figure 4. The microwave

radiation device consists of a magnetron, a rectangular metal waveguide, and a resonant cavity. The microwave can be excited by the magnetron and then radiated to the concrete specimen through the waveguide and the resonant cavity. The power of the magnetron is 1000 W. The temperature measurement device includes an optical-fiber temperature sensor and the FLIR ONE PRO/LT infrared thermal imager. The optical-fiber temperature sensor and paperless recorder are used to monitor and record the temperature during microwave irradiation. The temperature measurement range of the optic fiber temperature sensor is from –20 to 210 °C; measurement accuracy is 0.5% ± 1 °C, and the resolution is 0.1 °C. In addition, in order to obtain more comprehensive and detailed temperature information, the infrared thermal imager is used for real-time temperature measurement.

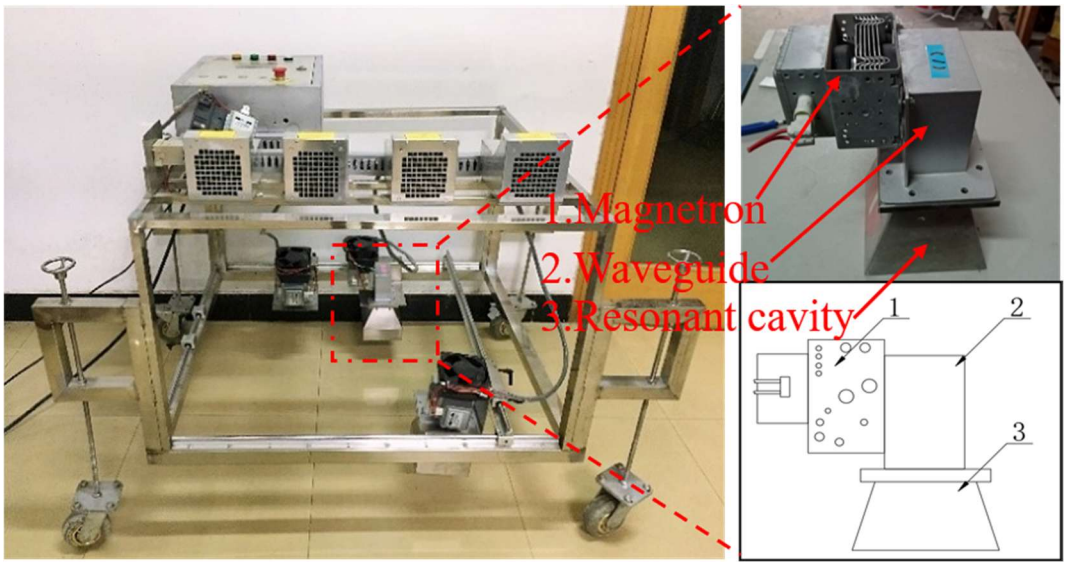

Figure 4. Open microwave deicing system.

2.2.2. Resistivity test system

The resistivity test system is comprised of the HY3005 MT DC regulated power supply, MT-1280 multimeter, and wire, as shown in Figure 5.

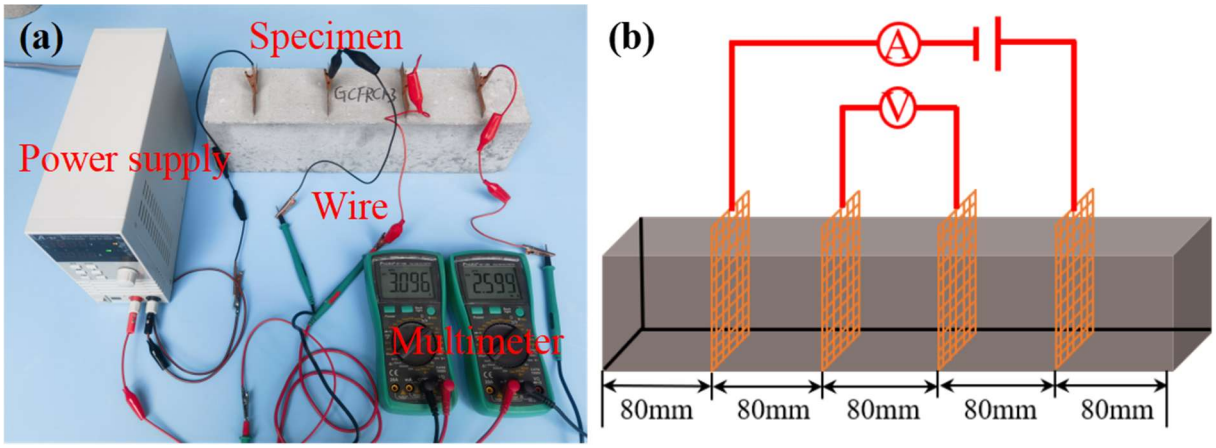

Figure 5. Resistivity test system. (a) Physical picture and (b) schematic diagram**.**

2.2.3. Electromagnetic parameter test system

The electromagnetic parameter test system is shown in Figure 6. The ROHDE & SCHWARZÂ ® ZND dual-port vector network analyzer can be used in the frequency range of 100 kHz to 4.5 GHz. The special test fixture for the electromagnetic concrete parameter can be used for continuous sweep frequency test of materials. The test range of electromagnetic parameters is $\varepsilon' = 2–100$ and $\varepsilon'' = 0.2–200$.

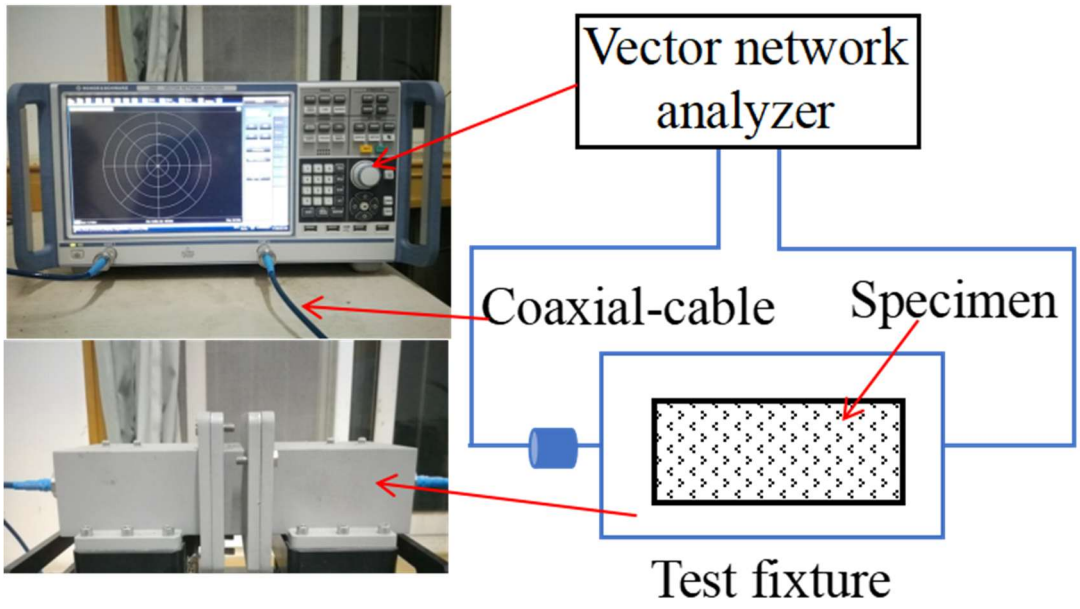

Figure 6. Electromagnetic parameter test system.

2.3. Test scheme

2.3.1. Ice-free heating test

The open microwave deicing system is used to irradiate the specimens without an ice layer; the distance from the microwave source to the specimen surface is 20 mm, and the microwave irradiation time is 80 s. The temperature sensor is used to monitor and record the temperature, and the real-time temperature rise curve is obtained. After microwave irradiation, the surface thermal image of the specimen without an ice layer is taken by the infrared thermal imager, and the temperature distribution of the specimen is analyzed. Each group of specimens undergoes three valid tests, and the average value of the results is calculated.

2.3.2. Microwave deicing test

The distance from the microwave source to the ice layer surface is 20 mm. The open microwave deicing system is used to irradiate the specimen with an ice layer for 100 s to observe the melting of the ice layer. Then, floating ice is removed, and the shape and area of the ice-breaking region are observed and measured. The typical shape and area of the ice-breaking region will be compared. Each group of specimens undergoes three valid tests, and the average value of the results is calculated.

2.3.3. Resistivity test

According to the "four electrode method", the resistivity test system is used to test the resistivity of the specimen, and a copper mesh is used as the electrode. When the specimen is prepared, four copper mesh electrodes are pre-embedded at equal intervals. The diameter of the copper mesh monofilament is 1 mm, and the test voltage is 10 V. Each group of specimens undergoes three valid tests, and the average value of the results is calculated.

2.3.4. Electromagnetic parameter test

The electromagnetic parameters of CNFsRC and CFsRC are tested using the electromagnetic parameter test system. The test frequency range is 2.35–2.55 GHz, and the microwave loss characteristics of CNFsRC and CFsRC are investigated. Each group of specimens undergoes three valid tests, and the average value of the results is calculated.

3. Results and discussion

3.1. Temperature rise rate

The time-temperature curve of CNFsRC is shown in Figure 7a, and the temperature rise rate (R_T) of CNFsRC and CFsRC is shown in Figure 7b. From these figures, it can be seen that the time-temperature curve of CNFsRC is approximately linear. The addition of CNFs does not affect the time-temperature concrete curve law, and there is no "temperature step" [23].

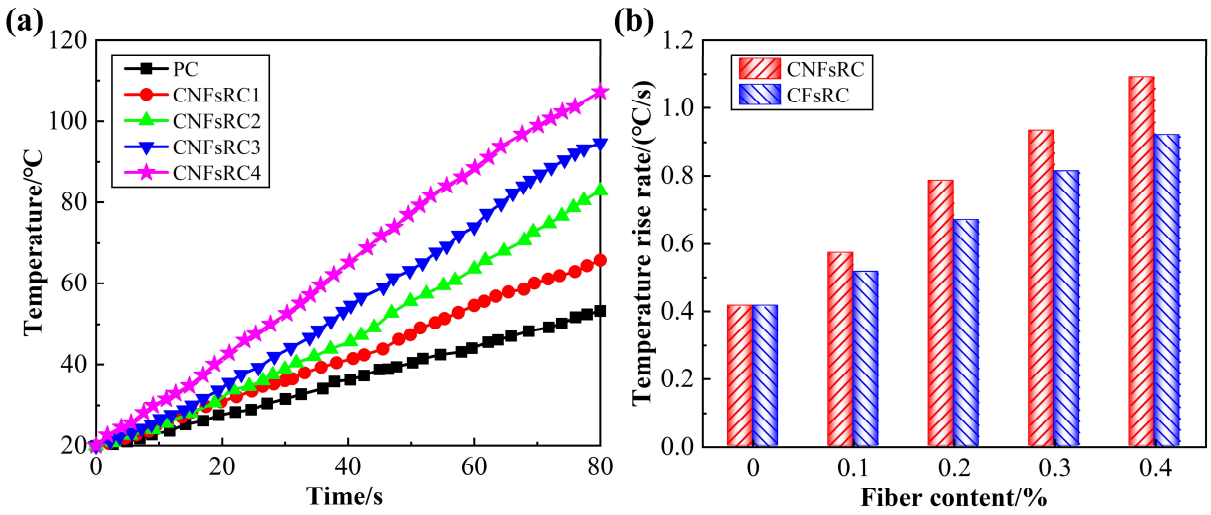

Figure 7. Time-temperature curve and temperature rise rate of concrete. (a) Time-temperature curve of CNFsRC; (b) temperature rise rate of CNFsRC and CFsRC.

CNFs can effectively improve the microwave heating rate of concrete. As the CNF content increases, the microwave heating rate increases. After microwave irradiation for 80 s, the temperature rise range of PC is only 33.1 °C, and the temperature rise range of CNFsRC1–CNFsRC4 is 45.7, 62.8, 74.7, and 87.3 °C, respectively. Figure 7 shows that the addition of CNFs and CFs can

increase the R_T of concrete during microwave irradiation, and as the CNFs and CFs increase, the R_T of CNFsRC and CFsRC increases. When the CNFs and CFs content is 0.4%, the R_T of CNFsRC4 and CFsRC4 are 1.09 °C/s and 0.92 °C/s, respectively, increasing by 162.89% and 121.93%, respectively. When the content of CNFs and CFs is the same, the R_T of CNFsRC is larger than that of CFsRC. From this, compared with CFs, CNFs have a better improvement effect on the microwave heating rate of PC.

3.2. Temperature distribution

The infrared thermal images of surface CNFsRC and CFsRC are shown in Figure 8. The shape of the heating region of CNFsRC and CFsRC is the same as that of PC, related to the microwave transmission characteristics of rectangular waveguides. By comparing the color of the central region of these infrared images, we find that CNFs can improve the heating effect of concrete. The larger the CNFs content, the better this heating effect. When the CNFs content is 0.4%, the central region of CNFsRC4 appears partially white, indicating that the temperature of the central region of CNFsRC4 reaches the maximum, consistent with the conclusion of the temperature rise curve. Compared with PC, the area of the heating region of CNFsRC and CFsRC is larger. The addition of CNFs and CFs can increase the heating region area. As the CNFs content increases, the heating region area of CNFsRC increases. In addition, although the heating region area of CNFsRC4 has a certain expansion, it still cannot increase the surface temperature of the whole specimen; that is, there is a clear heating boundary during microwave irradiation [34].

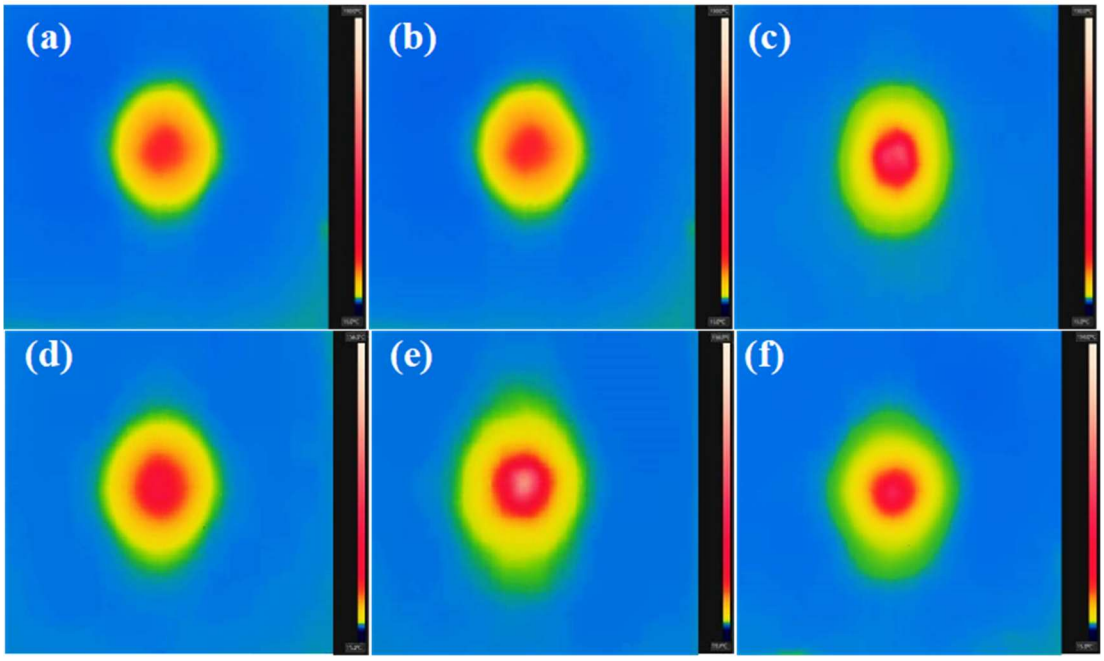

Figure 8. Infrared thermal images of the surfaces of CNFsRC and CFsRC. (a) PC; (b) CNFsRC1; (c) CNFsRC2; (d) CNFsRC3; (e) CNFsRC4; and (f) CFsRC4.

According to Figure 8, the three-dimensional temperature distribution picture of the surface of the specimens can be drawn, as shown in Figure 9. The three-dimensional temperature distribution pictures of CNFsRC and CFsRC show a cone shape with an elliptical planar substrate. Compared

with PC, the height of the cones of CNFsRC and CFsRC increases significantly. After the addition of CNFs and CFs, the dispersed fibers contact each other inside the concrete and form a conductive network structure. The electrical conductivity and polarization degree of the concrete are improved by CNFs and CFs, and the electromagnetic wave energy is more easily absorbed and converted into heat energy. On the macro level, the temperature of CNFsRC and CFsRC significantly increases. The heating region area of concrete is proportional to the heating rate, and the heating rate and heating region area of CNFsRC are larger than those of PC and CFsRC. According to the heat conduction principle and Fourier's law, the heat transfer rate of an object is proportional to the temperature gradient and thermal conductivity. For CNFsRC, the temperature rise rate is larger, so the corresponding heat flux density is also larger. Therefore, CNFsRC has a faster rate of heat transfer to the edge and a larger heating region area.

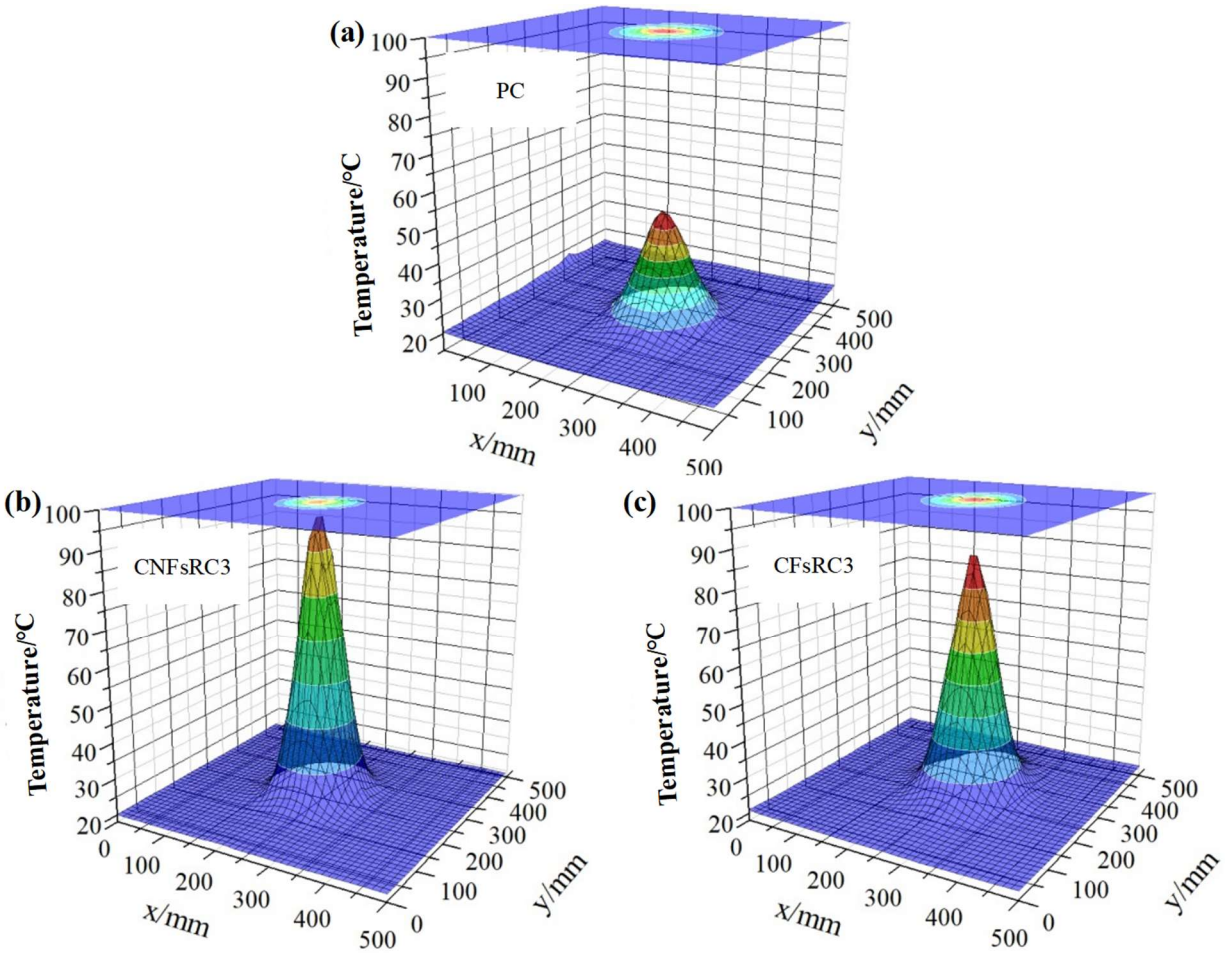

Figure 9. Three-dimensional temperature distribution of CNFsRC and CFsRC. (a) PC; (b) CNFsRC3; and (c) CFsRC3.

3.3. Microwave deicing efficiency

The microwave deicing efficiency of CNFsRC and CFsRC is shown in Figure 10. After microwave heating for 100 s, the ice-breaking region area of PC is 82.7 mm^2. CNFs can improve this parameter. When the CNFs content is 0.1%–0.4%, the ice-breaking region area of the concrete

is 110.3, 128.5, 140.8, and 180.9 mm^2, respectively, an increase by 33.37%, 55.38%, 70.25%, and 118.74%, respectively. The ice-breaking region area of CFsRC4 increases by 99.76% compared with that of PC, but it is smaller than that of CNFsRC. CFs can also improve the ice-breaking region area of concrete, but such improvement is lower. The shapes of the ice-breaking region of PC, CNFsRC, and CFsRC are elliptical. The shape of the ice-breaking region is determined by the electromagnetic field structure of the rectangular waveguide and is independent of the addition of fibers and fiber content [35]. On the rectangular cross-sections in the rectangular waveguide, the electric field is sinusoidally distributed along the wide side of the waveguide, while it is uniformly distributed along the narrow side of the waveguide [36]. The closer to the edge of the wide side of the waveguide, the weaker the electric field intensity. The spatial distribution of the electric field affects the distribution of microwave intensity; as such, the heating region and the ice-breaking region of the concrete are ellipsoids. The heating and ice-breaking regions are strongly elliptical due to waveguide effects. The multi-wave-source microwave deicing technology is explored in an attempt to solve this problem.

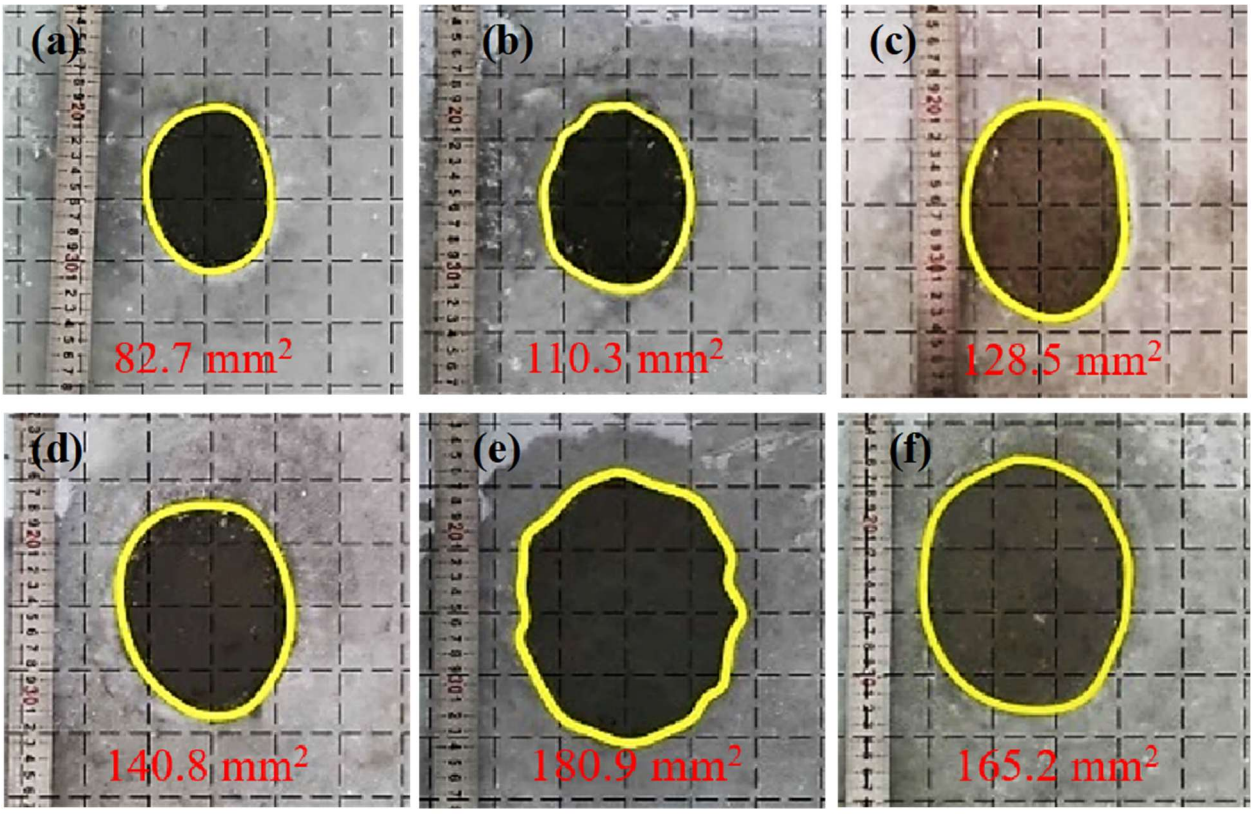

Figure 10. Microwave deicing efficiency of CNFsRC and CFsRC. (a) PC; (b) CNFsRC1; (c) CNFsRC2; (d) CNFsRC3; (e) CNFsRC4; and (f) CFsRC4.

3.4. Resistance loss characteristics

The resistivity (R) of CNFsRC and CFsRC is shown in Figure 11. Both CNFs and CFs can decrease the R and improve the conductivity of PC. As CNFs and CFs content increases, the conductivity of CNFsRC and CFsRC increases. When the CNFs and CFs content is 0.4%, the R of CNFsRC4 and CFsRC4 decreases by 28.47% and 37.60%, respectively. When the content of CNFs

and CFs is the same, the *R* of CFsRC is lower, and the conductivity of CFsRC is stronger than that of CNFsRC. Compared with CNFs, CFs have a better improvement effect on the conductivity of concrete. Both CNFs and CFs are carbon-based fibers with excellent electrical conductivity [37]. Therefore, CNFs and CFs can decrease the *R* of PC and improve the conductivity of PC. Compared with CNFs, CFs have a larger length-to-diameter ratio and a better bonding degree between fibers, making it easier to form a conductive network inside concrete [38]. Therefore, the conductivity of CFsRC is stronger than that of CNFsRC.

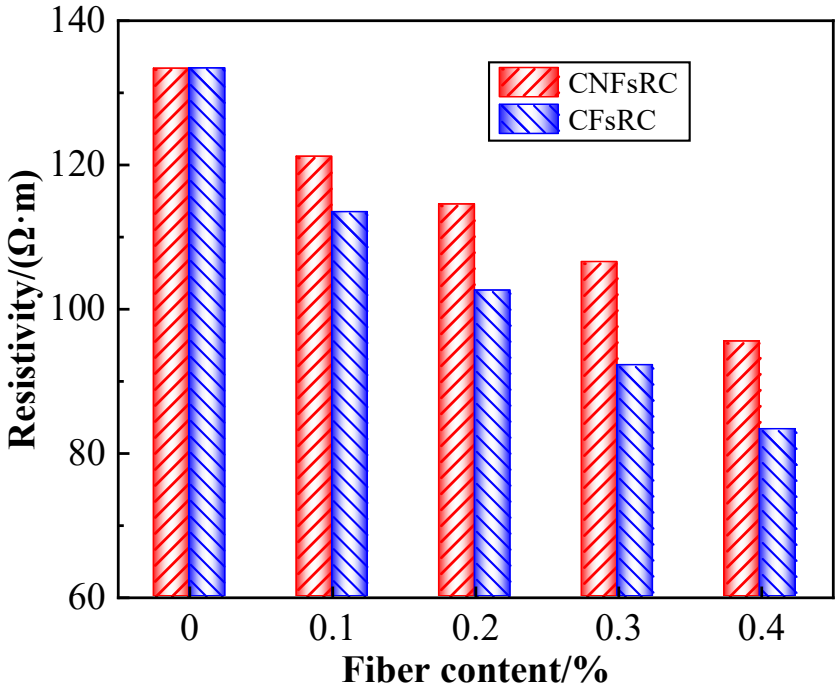

Figure 11. Resistivity of CNFsRC and CFsRC.

By improving the conductivity of concrete, CNFs and CFs enhance the resistance loss ability of concrete. When the electromagnetic wave enters concrete, as resistance-loss materials, CNFs and CFs can generate a current to heat the resistance material, resulting in the generation of thermal energy [39]. CNFs and CFs improve the microwave deicing efficiency by improving the resistance loss characteristics of concrete. In addition, the better the conductivity of the material, the more electromagnetic waves the material reflects [40]. Although CFsRC has better conductive and resistance loss characteristics, it reflects more electromagnetic waves. Therefore, the electromagnetic wave energy entering CFsRC is low, which is not conducive to wave absorption. The *R* of CNFsRC is lower than that of CFsRC, and its resistance loss characteristic is weaker than that of CFsRC, but CNFsRC can absorb more electromagnetic energy [41]. Therefore, CNFsRC shows better microwave deicing efficiency.

3.5. Dielectric loss characteristics

The complex dielectric constant (ε', ε'') is composed of a real and an imaginary part. The ε' and ε'' represent the polarization capacity and energy loss capacity of concrete in the electromagnetic field, respectively. The dielectric loss angle tangent $tan\delta_\varepsilon = \varepsilon''/\varepsilon'$ characterizes the dielectric loss

capacity of concrete [28]. The ε'' and $tan\delta_\varepsilon$ are positively correlated with dielectric loss characteristics. The ε' of CNFsRC and CFsRC is shown in Figure 12, where we can see that the ε' of CNFsRC and CFsRC is larger than that of PC. For 2.35–2.55 GHz, as the CNF content increases, the ε' of CNFsRC and the polarization ability of CNFsRC increase. When the CNF content is 0.4%, the ε' of concrete reaches the maximum, which is 28.21–29.23, increasing by 299.01%–352.63% compared with that of PC. The ε' of CFsRC4 is 21.48–21.73, increasing by 199.58%–236.37% compared with that of PC. Compared with CFsRC4, the ε' of CNFsRC4 is larger. Compared with CFs, CNFs have a better improvement in the polarization ability of PC.

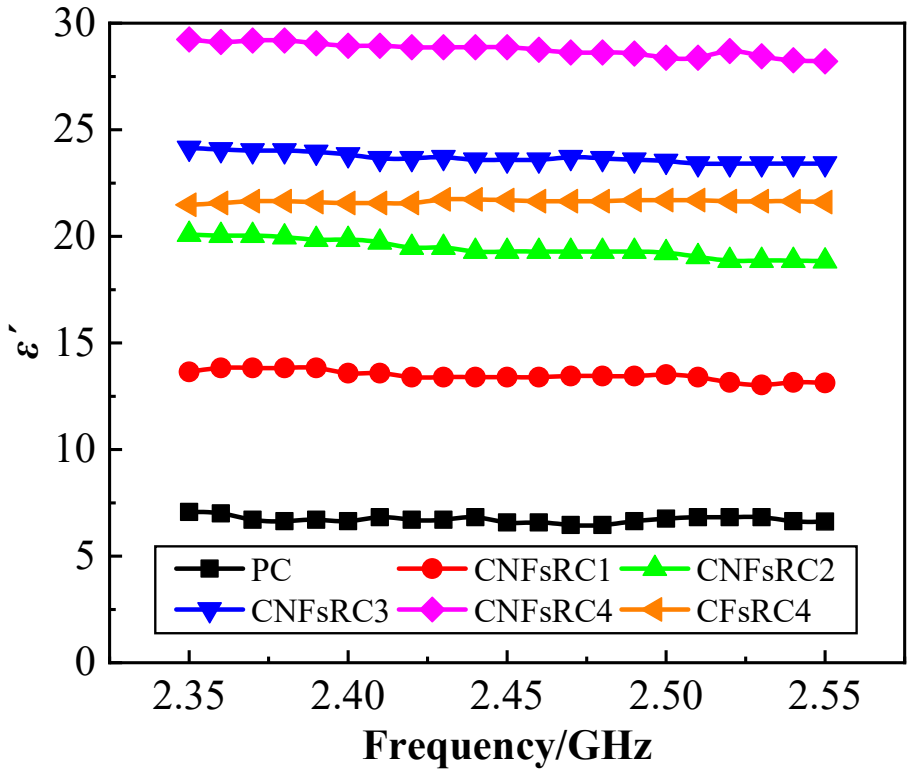

Figure 12. The ε' of CNFsRC and CFsRC.

The ε'' and $tan\delta_\varepsilon$ of CNFsRC and CFsRC are shown in Figures 13. The variation of ε'' and $tan\delta_\varepsilon$ of CNFsRC is consistent with that of ε'. For 2.35–2.55 GHz, CNFs can improve the ε'' and $tan\delta_\varepsilon$ of PC. This shows that CNFs can improve the dielectric loss characteristics of PC, and CNF is a good microwave attenuation material. When the CNF content is 0.4%, the ε'' and $tan\delta_\varepsilon$ of concrete are the maximum, and the dielectric loss ability is the strongest. The ε'' and $tan\delta_\varepsilon$ of PC are 0.50–1.34 and 0.08–0.20, respectively, while the ε'' and $tan\delta_\varepsilon$ of CNFsRC4 are 24.25–24.50 and 0.83–0.86, respectively. The dielectric loss capacity is the basis for the microwave heating efficiency of concrete. In the ice-free heating and microwave deicing tests, the heating efficiency and deicing effect of CNFsRC4 are the best, consistent with this conclusion. Compared with CFsRC4, the ε'' and $tan\delta_\varepsilon$ of CNFsRC4 are larger, and the dielectric loss capacity of CNFsRC4 is stronger. This shows that CNFs have a better improvement in the microwave loss characteristics of PC.

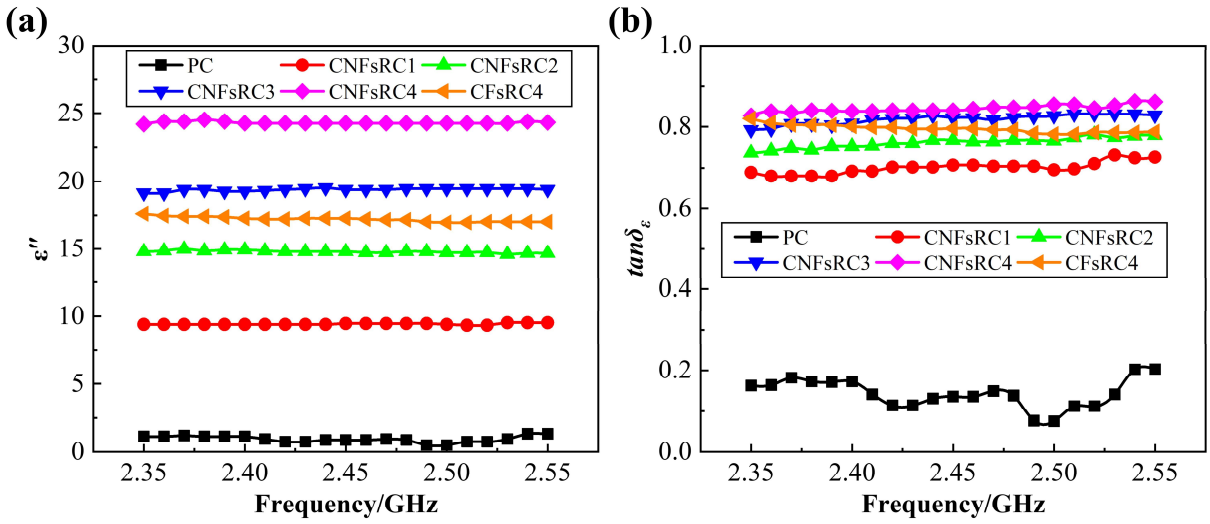

Figure 13. Imaginary part ε'' of complex dielectric constant and dielectric loss angle tangent $tan\delta_\varepsilon$ *of* CNFsRC and CFsRC. (a) Imaginary part ε'' of complex dielectric constant and (b) dielectric loss angle tangent $tan\delta_\varepsilon$.

As dielectric loss materials, CNFs and CFs can improve the dielectric loss capacity of PC. In the concrete mixed with CNFs and CFs, these can be regarded as dipoles. CNFs dipoles and CFs dipoles can also polarize in an electromagnetic field and convert electromagnetic wave energy into thermal energy. After the addition of CNFs and CFs, the number of dipoles in concrete increases, so the polarization ability and dielectric loss capacity of CNFsRC and CFsRC are improved [28,42]. Therefore, the ε', ε'', and d $tan\delta_\varepsilon$ of CNFsRC and CFsRC are larger than those of PC. During microwave irradiation, the heating power P of concrete is shown in Eq 1:

$$P = \frac{0.566 \times 10^{-10}}{c\rho} f\varepsilon'' E_{rms}^2 \tag{1}$$

where c is the velocity of light, ρ is the density, f is the wavelength of the microwave, and E_{rms} is the maximum electric field intensity inside the concrete. From Eq 1, the heating power P of concrete is proportional to the imaginary part ε''. After the addition of CNFs and CFs, the imaginary part ε'' of concrete increases, and the microwave heating and deicing efficiencies of CNFsRC and CFsRC are improved. The imaginary part ε'' of CNFsRC4 is larger than that of CFsRC4, so the microwave heating and deicing efficiency of CNFsRC4 is better.

In an early stage, the effect of CNFs on the mechanical properties of concrete was studied. When the CNF content was 0.1%–0.4%, the strength of CNFsRC was larger than that of plain concrete; when the CNF content was 0.5%, the strength of CNFsRC was smaller than that of plain concrete [43,44].

4. Conclusions

The microwave deicing efficiency and loss characteristics of CNFsRC and CFsRC are studied and compared. The main conclusions are as follows:

(1) CNFs can improve the microwave heating and deicing efficiency of concrete. As the CNFs content increases, the surface temperature, temperature rise rate, area of microwave heating region, and area of ice-breaking region of concrete increase.

(2) CNFs can reduce the resistivity of concrete and increase the complex permittivity real part, imaginary part, and dielectric loss angle tangent of concrete, thereby improving the resistance loss and dielectric loss characteristics of concrete.

(3) CNFs can improve the resistance loss and dielectric loss characteristics of concrete. The larger the CNF content, the better the microwave loss characteristics of concrete.

(4) The improvement of microwave deicing efficiency of concrete by CNFs is better than that by CFs. The resistance loss characteristic of CFsRC is better than that of CNFsRC, but the wave-absorption effect of CFsRC is poor, and the dielectric loss characteristic of CNFsRC is better than that of CFsRC.

Although the improvement in microwave deicing efficiency of concrete with CNFs is better than with CFs, CNFs are more expensive. In recent years, the production cost of CNFs has decreased, and the production scale has gradually expanded, which has broadened the application prospects of CNFs in concrete.

Microwaves directly act on the ice layer and the road surface, achieving high heating efficiency and reducing energy loss during the transmission process. Microwave deicing technology is feasible and has achieved interesting results in laboratory and small-scale tests. However, it is still in the development stage and faces some application limitations.

Use of AI tools declaration

The authors declare they have not used Artificial Intelligence (AI) tools in the creation of this article.

Acknowledgments

This study was funded by National Natural Science Foundation of China (Grant No. 52278287).

Author contributions

Zhihang Wang: Conceptualization, methodology, validation, writing-original draft; Binghong Li: Data curation, visualization, writing-review & editing; Chao Zhang and Yue Zhang: Project administration, investigation, visualization; Chao Wang: Validation; Erlei Bai: Investigation.

Conflict of interest

The authors declare no conflict of interest.

References

1. Chen H, Xu J, Wu Y, et al. (2020) Study on the thermodynamic properties of concrete surface uring microwave deicing of airport pavement. *Material* 13: 3557. https://doi.org/10.3390/ma13163557
2. Liu X, Zhao Y, Liu W, et al. (2022) Microwave heating and deicing efficiency for asphalt concrete with SiC-Fe_3O_4 microwave enhanced functional layer. *J Cleaner Prod* 332: 130111. https://doi.org/10.1016/j.jclepro.2021.130111
3. Gulisano F, Gallego J, Trigos L, et al. (2021) Dielectric characterisation of asphalt mortars for microwave heating applications. *Constr Build Mater* 308: 125048. https://doi.org/10.1016/J.CONBUILDMAT.2021.125048
4. Fakhri M, Javadi S, Sedghi R, et al. (2021) Microwave induction heating of polymer-modified asphalt materials for self-healing and deicing. *Sustainability* 13: 10129. https://doi.org/10.3390/SU131810129
5. Guo H, Wang Z, Huo J, et al. (2020) Microwave heating improvement of asphalt mixtures through optimizing layer thickness of magnetite and limestone aggregates *J Cleaner Prod* 273: 123090. https://doi.org/10.1016/j.jclepro.2020.123090
6. Ding L, Wang X, Cui X, et al. (2021) Development and performance research of new sensitive materials for microwave deicing pavement at different frequencies. *Cold Reg Sci Tech* 181: 103176. https://doi.org/10.1016/j.coldregions.2020.103176
7. Xu O, Han S, Liu Y, et al. (2020) Experimental investigation surface abrasion resistance and surface frost resistance of concrete pavement incorporating fly ash and slag. *Int J Pavement Eng* 22: 1858–1866. https://doi.org/10.1080/10298436.2020.1726348
8. Wang Z, He Z, Wang Z, et al. (2019) Utilization of magnetite as microwave absorber to prepare microwave-heatable aggregate for deicing in cementitious composite. *Constr Build Mater* 227: 116664. https://doi.org/10.1016/j.conbuildmat.2019.08.045
9. Zhang J, Yan Y, Hu Z, et al. (2018) Utilization of low-grade pyrite cinder for synthesis of microwave heating ceramics and their microwave deicing performance in dense-graded asphalt mixtures. *J Cleaner Prod* 170: 486–495. https://doi.org/10.1016/j.jclepro.2017.09.175
10. Liu X, Wei Z, Zhao Y, et al. (2021) Improving the electromagnetic properties of bitumen using SiC-Fe_3O_4 composites. *J Mater Civ Eng* 33: 04021326. https://doi.org/10.1061/(ASCE)MT.1943-5533.0003953
11. Gao J, Guo H, Wang X, et al. (2019) Microwave deicing for asphalt mixture containing steel wool fibers. *J Cleaner Prod* 206: 1110–1122. https://doi.org/10.1016/j.jclepro.2018.09.223
12. Guan B, Liu J, Zhao H, et al. (2019) Investigation of the microwave absorption of asphalt mixtures containing magnetite powder. *Coatings* 9: 813. https://doi.org/10.3390/coatings9120813
13. Liu Z, Yang X, Wang Y, et al. (2019) Engineering properties and microwave heating induced ice-melting performance of asphalt mixture with activated carbon powder filler. *Constr Build Mater* 197: 50–62. https://doi.org/10.1016/j.conbuildmat.2018.11.094
14. Wang Z, He Z, Wang Z, et al. (2019) Microwave deicing of functional pavement using sintered magnetically separated fly ash as microwave-heating aggregate. *J Mater Civ Eng* 31: 04019127. https://doi.org/10.1061/(ASCE)MT.1943-5533.0002771

15. Ding L, Wang X, Zhang W, et al. (2018) Microwave deicing efficiency: Study on the difference between microwave frequencies and road structure materials. *Appl Sci* 8: 2360. https://doi.org/10.3390/app8122360
16. Ouyang W, Wang Z, Zhang C, et al. (2025) Electromagnetic shielding and wave absorbing properties of graphene oxide grafted carbon fiber reinforced concrete. *Fuller Nanotub Carbon Nanostruct* 33: 1201–1213. https://doi.org/10.1080/1536383X.2025.2495813
17. Zhao J, Gao Z, Wu W, et al. (2025) Development of a novel cement-based microwave deicing functional overlay using waterborne epoxy resin: Heating properties, influencing factors, and mechanism. *Constr Build Mater* 492: 142849. https://doi.org/10.1016/J.CONBUILDMAT.2025.142849
18. Chen T, Liu J, Wang G, et al. (2025) Experimental study on multi-source coupled microwave deicing of pavement concrete. *Constr Build Mater* 499: 144074. https://doi.org/10.1016/J.CONBUILDMAT.2025.144074
19. Liu J, Xu J, Lu S, et al. (2019) Investigation on dielectric properties and microwave heating efficiencies of various concrete pavements during microwave deicing. *Constr Build Mater* 225: 55–66. https://doi.org/10.1016/j.conbuildmat.2019.07.249
20. Wang Z, Bai E, Ren B, et al. (2023) Microwave heating efficiency and frost resistance of concrete modified with powder absorbing materials. *Constr Build Mater* 379: 131145. https://doi.org/10.1016/J.CONBUILDMAT.2023.131145
21. Lu S, Bai E, Xu J, et al. (2021) Research on electromagnetic properties and microwave deicing performance of carbon fiber modified concrete. *Constr Build Mater* 286: 122868. https://doi.org/10.1016/J.CONBUILDMAT.2021.122868
22. Liu J, Xu J, Lu S (2017) Investigations on microwave deicing effects on graphite-modified concrete. *RSC Adv* 7: 39237–39243. https://doi.org/10.1039/c7ra04920j
23. Wang Z, Bai E, Huang H, et al. (2022) Study on the electromagnetic property and microwave heating efficiency of concrete with magnetite aggregate. *Constr Build Mater* 342: 128080. https://doi.org/10.1016/J.CONBUILDMAT.2022.128080
24. Wang Z, Bai E, Ren B, et al. (2024) Mechanical properties and cross-scale synergistic modification mechanism of micro-nano carbon fiber modified concrete. *Mater Today Commun* 2024: 110401. https://doi.org/10.1016/J.MTCOMM.2024.110401
25. Wang Z, Bai E, Liu J, et al. (2025) Research progress on electromagnetic shielding and wave absorption properties of cement-based materials modified by carbon fiber and carbon nanomaterials. *Mater Rep* 39: 88–96. https://doi.org/10.11896/cldb.24030248
26. Du Y, Wang Z, Lu S, et al. (2025) Mechanical characteristics of multi-scale carbon nanotube-carbon fiber reinforced concrete and a dynamic constitutive model within an EP damage framework. *Case Stud Constr Mater* 23: e05616. https://doi.org/10.1016/J.CSCM.2025.E05616
27. Qiu H, Wu Y, Chen H, et al. (2023) Effect of silicon carbide powder on temperature field distribution characteristics and microwave deicing efficiency of cement concrete containing magnetite (Fe_3O_4) powder. *Constr Build Mater* 392: 132005. https://doi.org/10.1016/J.CONBUILDMAT.2023.132005
28. Bai E, Wang Z, Du Y, et al. (2024) Mechanical properties and strain rate effect of graphene oxide grafted carbon fiber modified concrete under dynamic impact load. *Constr Build Mater* 445: 137978. https://doi.org/10.1016/J.CONBUILDMAT.2024.137978

29. Wang Z, Bai E, Liu C, et al. (2024) Strength, toughness and interface modification of graphene oxide grafted carbon fiber modified concrete. *Constr Build Mater* 428: 136336. https://doi.org/10.1016/J.CONBUILDMAT.2024.136336
30. Wang Z, Bai E, Liang L, et al. (2024) Comparison of dynamic mechanical properties of carbon fiber and graphene oxide grafted carbon fiber modified concrete. *J Build Eng* 94: 109989. https://doi.org/10.1016/J.JOBE.2024.109989
31. Kumar A, Sachdev VK, Chowdhuri A, et al. (2023) Electromagnetic shielding effectiveness and dielectric study of polystyrene/aluminum composite by addition of graphite and carbon nanofiber powder. *J Mater Sci-Mater Electron* 34: 11232. https://doi.org/10.1007/S10854-023-11232-W
32. Liu M, Hu J, Wang H, et al. (2023) 3D flower-branch hierarchical carbon nanofiber/ZnO/TiO_2/$Ti_3C_2T_x$ composites for dramatically enhanced electromagnetic absorbing properties. *Ceram Int* 49: 34062–34073. https://doi.org/10.1016/J.CERAMINT.2023.08.107
33. Xia W, Bai E, Lu S, et al. (2023) Optimal design and experimental study of horn antenna in pavement microwave deicing technology. *Cold Reg Sci Tech* 205: 103695. https://doi.org/10.1016/J.COLDREGIONS.2022.103695
34. Liu K, Da Y, Wang F, et al. (2022) An eco-friendly asphalt pavement deicing method by microwave heating and its comprehensive environmental assessments. *J Cleaner Prod* 373: 133899. https://doi.org/10.1016/J.JCLEPRO.2022.133899
35. Ning Y, Xu J, Huang H, et al. (2022) Effect of carbon fiber admixture and length on microwave deicing efficiency of airport road surface concrete. *Adv Mater Sci Eng* 2022: 1956040. https://doi.org/10.1155/2022/1956040
36. Lu S, Xu J, Bai E, et al. (2017) Investigating microwave deicing efficiency in concrete pavement. *RSC Adv* 7: 9152–9159. https://doi.org/10.1039/c6ra27109j
37. Yoo D, Kang M, Choi H, et al. (2020) Influence of chemically treated carbon fibers on the electromagnetic shielding of ultra-high-performance fiber-reinforced concrete. *Arch Civ Mech Eng* 20: 602–610. https://doi.org/10.1007/s43452-020-00117-y
38. Han J, Wang D, Zhang P (2020) Effect of nano and micro conductive materials on conductive properties of carbon fiber reinforced concrete. *Nanotechnol Rev* 9: 445–454. https://doi.org/10.1515/ntrev-2020-0034
39. Liu X, Zhao Y, Yan D, et al. (2023) An environmentally friendly asphalt concrete containing SiC aggregate for microwave heating deicing. *J Mater Civ Eng* 35: 16230. https://doi.org/10.1061/JMCEE7.MTENG-16230
40. Ma L, Wu Y, Wu Z, et al. (2023) Enhanced dielectric loss in N-doped three-dimensional porous carbon for microwave absorption. *Mater Today Adv* 20: 100434. https://doi.org/10.1016/J.MTADV.2023.100434
41. Chen T, Wang Z, Zhang C, et al. (2025) Electromagnetic properties of carbon nanofiber reinforced concrete and comparison with carbon fiber reinforced concrete. *Fuller Nanotub Carbon Nanostruct* 33: 819–828. https://doi.org/10.1080/1536383X.2025.2463478
42. Lu D, Jiang X, Leng Z, et al. (2023) Dual responsive microwave heating-healing system in asphalt concrete incorporating coal gangue and functional aggregate. *J Cleaner Prod* 422: 138648. https://doi.org/10.1016/J.JCLEPRO.2023.138648

43. Chen T, Wang Z, Wang A, et al. (2023) Comparative study on the static and dynamic mechanical properties and micro-mechanism of carbon fiber and carbon nanofiber reinforced concrete. *Case Stud Constr Mater* 18: e01827. https://doi.org/10.1016/j.cscm.2023.e01827
44. Wang T, Xu J, Bai E, et al. (2023) Research on a sustainable concrete synergistic reinforced with carbon fiber and carbon nanofiber: Mechanical properties, durability and environmental evaluation. *Int J Hydrog Energy* 48: 35366–35386. https://doi.org/10.1016/J.IJHYDENE.2023.05.234

AIMS Press

© 2026 the Author(s), licensee AIMS Press. This is an open access article distributed under the terms of the Creative Commons Attribution License (http://creativecommons.org/licenses/by/4.0)